AN ULTRASONIC GLOBAL INSPECTION TECHNIQUE FOR AN OFFSHORE K-JOINT

Submitted to

The Society of Petroleum Engineers

By

Joseph L. Rose
Yi H. Jeong
Michael J. Avioli

at

Ultrasonics Research Laboratory
Drexel University
Philadelphia, PA

on

May 1, 1981

ABSTRACT

Offshore steel platforms are used for drilling and the production of oil and gas. Inspection of offshore structural damage has been carried out by either divers or remote-controlled submersibles. However, these are severely limited by the prevailing weather or water state. In silty, muddy, or highly turbulent water, the visual inspections by divers, TV camera, or magnetic particles, can not be carried out successfully. What's more, the manual inspection by divers is, even under good conditions, extremely difficult in deep water and takes a great deal of time and money.

In order to overcome these difficulties, AN ULTRASONIC GLOBAL INSPECTION TECHNIQUE was developed for detecting damage in a K-Joint. This technique is based upon early detection of the signal change caused by various damage in the pipe weld. The signal change can be detected by SIMILARITY COEFFICIENT ANALYSIS.

Three major efforts were made throughout the project for three different scale K-Joint models; 1/19, 1/10 and 1/3 scale models*.

It should be noted that even complete individual joint failure does not necessarily lead to failure of the entire platform. The important philosophy of this approach is to detect any major damages early enough to repair them before complete failure of the joint. From this viewpoint, AN ULTRASONIC GLOBAL INSPECTION TECHNIQUE was able to detect the damages early enough to prevent any serious failures occurring on K-Joint models.

Finally, considering its performance and the simplicity of the test procedures, THE ULTRASONIC GLOBAL INSPECTION TECHNIQUE might be most promising and could adequately satisfy the requirements for offshore structural damage inspection. This project has been carried out as a part of THE OFFICE OF NAVAL RESEARCH PROGRAM.

Note; * For detailed informance, see Table 1.

2. PLATFORM DESIGN AND DAMAGE ANALYSIS

Piled steel platform consists of three major components: the jacket, the piling, and the deck. Gravity loads from drilling and deck weight are supported by the piling, which is driven into the sea bed. Deck sections are set directly into the piling. The jacket serves to provide a template for field installation, to provide lateral restraint to the piling, and to transfer lateral forces due to wind and wave to the piling. It consists of multiple legs interconnected by a series of horizontal, vertical, and diagonal braces. The places where the jacket brace members are joined are called nodes or joints. Typical joints are shown in Figure 1.

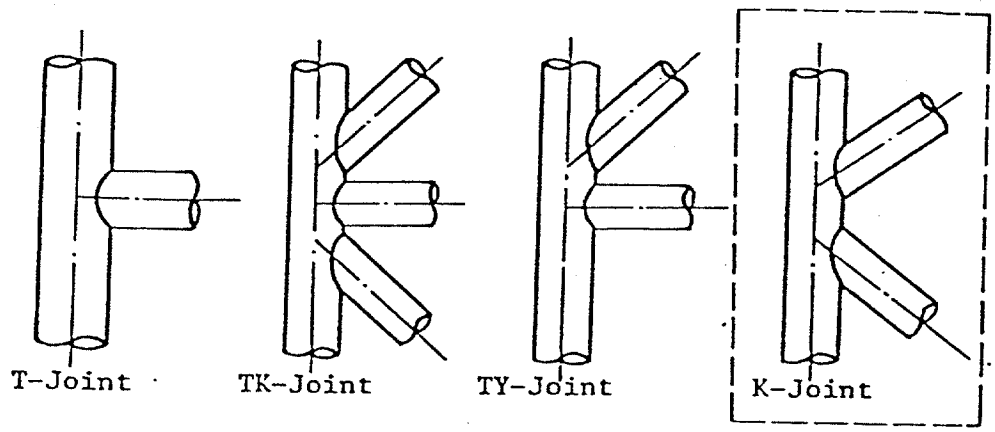

Figure 1. Typical Joint Configurations
(Follow AWS Structural Welding Code)

Nodes are points of high stress on the platform because stress concentrations occur due to the complex geometry in these intersections. Finite element analysis of these complicated shapes points up the existence of "Hot Spot" stress locations, generally at the top, bottom, and sides of the intersection. In actual welded joints, the profiles produced by welding cause the point of maximum stress to exist at the edge of the weld, as indicated in Figure 2.

1. INTRODUCTION

Due to the severe environmental conditions in the ocean such as continuous water waves, storms, marine growth, corrosion by water, etc., there have been numerous structural failures and catastrophic accidents on offshore platforms. Most of the failures, however, were found to be caused by damages to the welded pipe joints of the structural members. Up to the present, a number of inspection methods have been used for the detection of the damage to welded joints. However, those inspection methods have not been fully satisfactory to users because of their drawbacks in high cost and time consumption.

An ultrasonic global inspection technique will detect any serious damages occurring on K-joints with relatively low expense, low manpower and real time analysis. This technique was carried out by analyzing the ultrasonic signal travelling around the pipe wall. The ultrasonic transducer can possibly be attached permanently on the outside surface of the suspected welded joints for the periodic damage checking.

Detailed research efforts are explained throughout the major contents of this report.

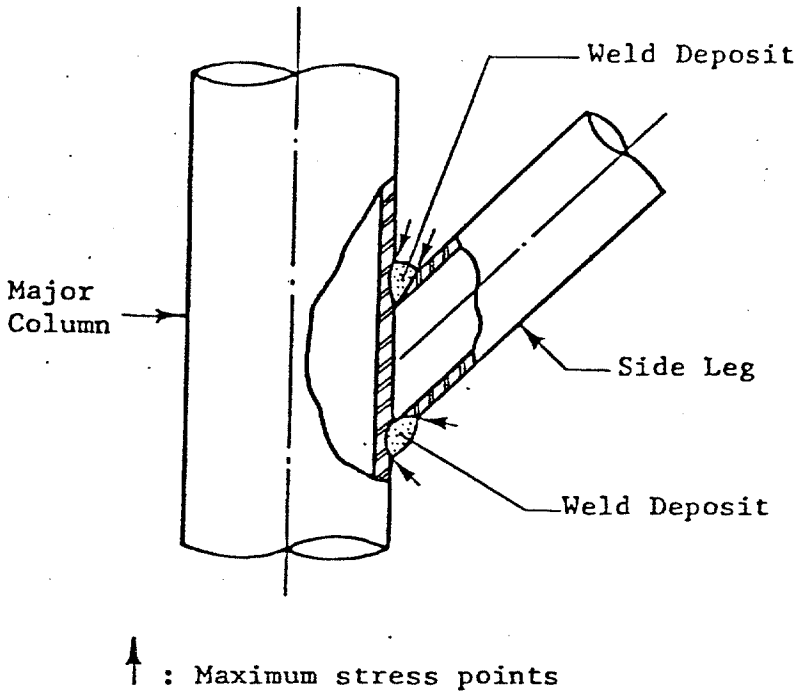

Figure 2. Typical Weld Profile for an Offshore Pipe Weld

Failure of a tubular joint, for the ultrasonic global inspection technique, will be considered to be the point where there is a distinct change in ultrasonic signal travelling around the pipe node which will cause a drastic drop of the similarity coefficient. It should be stated again that even complete failure in a node does not necessarily imply structural danger directly to the overall platform. Platforms are highly redundant. However, the accumulation and/or further growth of these damages at various places might cause a potential danger to the entire offshore platform. To determine if overall structural integrity is threatened by these damages, a structural analysis must be made separately.

Note: Major part of this section was taken from ref. (1).

3. TEST GEOMETRY OF K-JOINT MODEL AND PROBE DESIGN

Because of the complexity of the K-joint weld and the numerous joints in a single offshore structure, a local inspection method, such as a pulse-echo technique, would be inefficient and costly. Instead, a global inspection method, such as a through-transmission technique, is more useful. Therefore, in order to obtain the global information of crack initiation as well as crack propagation on K-joint weld, a through-transmission technique was employed. An ultrasonic signal is transmitted into the pipe wall from one side of the node and received at the other side. Any physical damages inside the major column will interfere with ultrasonic beam propagation, and will result in a signal change ("delta signal"). The delta signal is the key feature from which the existence of any physical damage can be predicted. The optimum transducer (transmitter and receiver) position around the pipe would be the place where the damage can be detected most sensitively. The optimum beam angle can also be found by considering both the sound beam direction inside the pipe wall and the pipe size. The theory behind the above concepts is as follows:

If the reflected beam inside the pipe wall does not touch the internal wall, the small internal flaw would not be detectable. The sound beam should also cover the whole thickness of the pipe wall. Therefore, the angle, β, (see Figure 3), when the refracted beam is tangent at the point, T, will be the maximum angle we can choose for a certain size (t/D ratio) of a pipe. The angle, β, also indicates the shortest sound path around the pipe. Consequently, the maximum sound energy will then be received from this angle. The angle, β, varies with respect to t/D ratio where t is pipe wall thickness and D is the outside diameter of the pipe. The angle, β, is calculated by the following relationship;

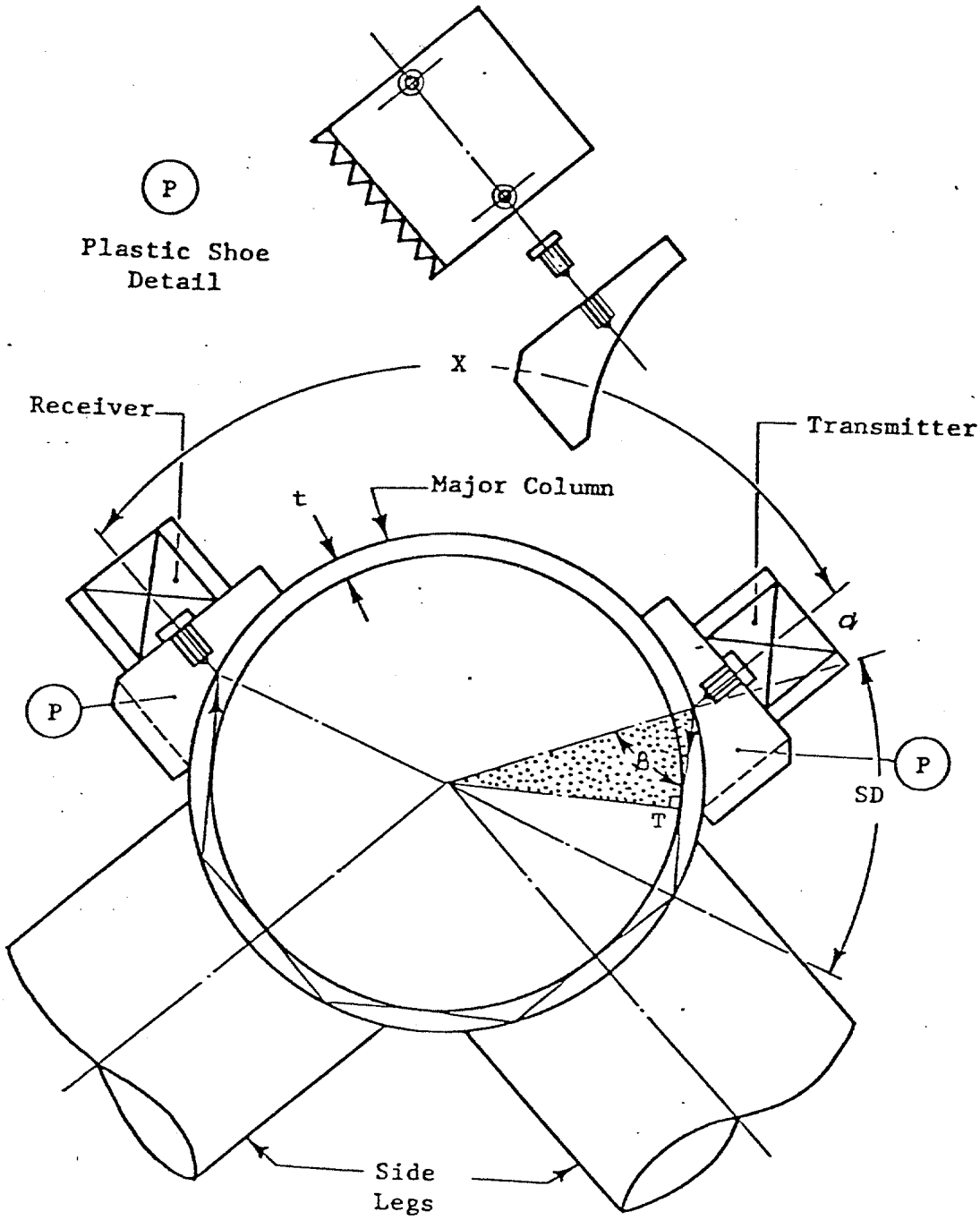

SD: Skip Distance
α: Angle of Incidence
β: Angle of Refraction

Figure 3. Cross Sectional View of K-Joint Model and Transducer Locations

$$\beta = \sin^{-1}\left[1 - 2(t/D)\right]$$

The complete table of the angle, β, for various t/D ratios is also available. From the angle, β, the angle of incidence, α, can be obtained using "Snell's Law";

$$\alpha = \sin^{-1}\left[\frac{C_{LS}}{C_{SM}} \times \left\{1 - 2(t/D)\right\}\right]$$

where C_{LS} - longitudinal wave velocity in the shoe material

C_{SM} - shear wave velocity in the medium

α - angle of incidence

t - pipe wall thickness

D - pipe outside diameter

Therefore, the optimum angle of incidence of the transducer is the angle, α.

In order to get the maximum sound energy, it is necessary to have the shortest sound path distance. In other words, especially for larger pipe, the transmitter and receiver should be placed as close to the side leg as possible in order to minimize the sound energy loss. Therefore, the optimum distance between transmitter and receiver would be the smallest number of multiples of the skip distance. The skip distance on pipe inspection is calculated by the formula

$$SD = \frac{\pi D}{180}(90 - \beta)$$

Therefore, the optimum distance (X) between transmitter and receiver is

$$\therefore X = \pi D - K \cdot SD$$

where K - smallest possible integer number dependent on the pipe size

X - optimum distance between transmitter and receiver (should not be interfered with side leg weld)

4. SCALING CONSIDERATION OF K-JOINT STRUCTURE FOR OPTIMUM TRANSDUCER SELECTION

Three major efforts were made throughout the project for three different scale K-joint models.

(1) Phase I; 1/19* Scale K-joint Model Study (at Drexel University)

(2) Phase II; 1/10* Scale K-joint Model Study (at Drexel University)

(3) Phase III; 1/3* Scale K-joint Model Study (at NASA)

Comments on structural and ultrasonic frequency scaling are summarized next.

Because of material availabilities, a series of models were prepared that were not a precise scale. These results are illustrated in Table 1. A number of things can be learned from these results along with a suggestion for the full scale model study.

Upon completion of Phase I and Phase II to illustrate versatility of the similarity coefficient, a series of studies were conducted to further examine the frequency selection criteria. It was found that as long as λ/thickness was between .2 and 1, frequency selection depended on penetration power, was strongly dependent on the pulser system used in the work. Two pulser systems were used in the work. Because KB-6000 pulser has a pulsing power more than four times as high as UTA-2 pulser, KB-6000 was chosen for larger pipe inspection. Therefore, UTA-2 was used for 1/19 and 1/10 scale K-Joint models and KB-6000 for 1/3 scale model. If the KB-6000 pulsers were used, however, higher frequencies could be used for the 1/19 or 1/10 models than those for UTA-2. Commercially available pulsers can handle frequencies greater than 700 kHz reliably. Also, the weld area surface condition(HAZ) of 1/3 scale model was better than those of 1/19 and 1/10 scale K-Joint models, consequently losing less sound energy.

Note; Physical dimensions are shown in Table 1.

Consideration of these realities, therefore, shows why 800 kHz on the KB-6000 was selected for the 1/3 scale K-Joint structure rather than 400 kHz which is the accurately scaled frequency. λ/t was equal to .22 which was good for resolution, being beyond the noise region and soundpath/λ was 313 which was suitable for the pulser unit. Since all of the tests in Phases I, II and III were successful, it can be anticipated that for the full scale λ/t should be maintained between .2 and 1 and soundpath/λ ratio less than 200 to 300, depending on the characteristics of the pulser that would be designed. Optimum frequency would therefore be somewhere between 250 and 500 kHz.

The fundamental transducer selection criteria for K-Joint inspection can, therefore, be summarized as shown in Table 2.

Table 2. Transducer Selection Criteria for K-joint Inspection

Resolution	λ/thickness < .1	-too sensitive and noisy
	λ/thickness > 1	poor resolution
Penetration	soundpath/λ > 400	too much loss in penetration (for KB6000)
	soundpath/λ > 150	(for UTA-2)

5. ULTRASONIC EQUIPMENT

The following ultrasonic equipment was used for this program.

The most important equipment in the data acquisition process is the Biomation 8100 transient recorder. The Biomation model 8100 has a maximum sampling rate of 100 MHz which permits better than ten samples per cycle for the estimated maximum frequency. According to sampling theory, the sampling rate must be at least twice the highest input frequency to be measured. In practical situations, any complex wave form, such as sine wave, should have at least five data point throughout the full cycle in order to adequately display the signal details. From this point of view, ten samples per cycle are sufficient to represent the sample wave form. Therefore, a reliable representation of the reflected signal should be obtained by 100 MHz sampling rate of the Biomation transient recorder.

A Hewlett Packard oscilloscope model 180D was used for supplementary display for the double checking of the exact digitized signal by the Biomation transient recorder.

A KB6000 ultrasonic data acquisition system was used as the pulser-receiver unit in order to get high power pulsing energy, enough to allow the ultrasonic waves to travel around the larger pipe. The KB-6000 unit was also specially tuned for low frequency transducer (800 KHz).

The microprocessor, LSI-11, was used for the signal processing and data acquisition.

A dual floppy unit, interfaced with LSI-11 microprocessor unit, was used for data storage.

The entire ultrasonic data acquisition system is shown in Figure 4.

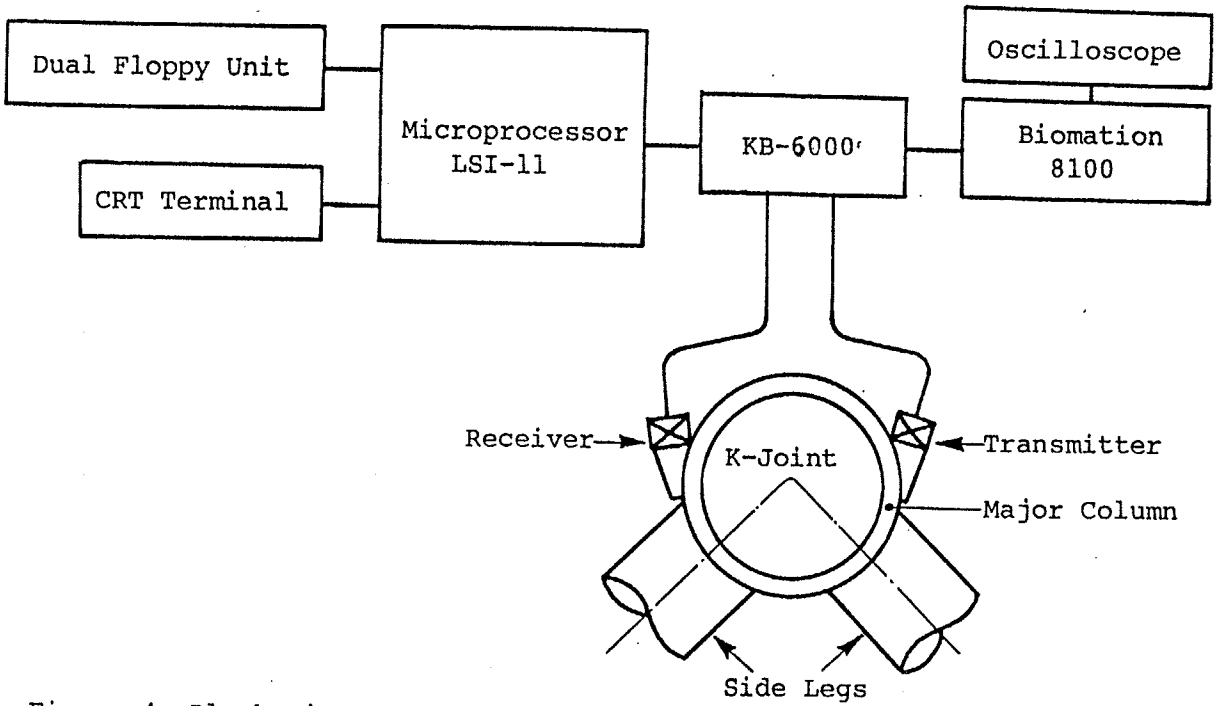

Figure 4. Block Diagram of Ultrasonic Data Acquisition System for K-Joint Model Study

6. SIMILARITY COEFFICIENT ANALYSIS

A similarity coefficient procedure was used for signal analysis. Consider the situation of two similar waveforms displaced different amounts from a time origin which happens frequently to the data acquisition process.

If it was desired to compare the similarity of these two waveforms, one of them would have to be shifted until it was, in a sense, in highest agreement with the other. The first step then is to eliminate this time delay effect. However, this problem can be eliminated by comparing the signals in frequency domain.

We can denote the first signal by f(t) and the second by $f(t-\mathcal{T})$ where $\mathcal{T}$ is the amount of phase shift. This is the ideal case where the signals are identical but displaced in time relative to each other. Taking Fourier transforms we have

$$\mathcal{F}[f(t-\mathcal{T})] = e^{-j\omega\mathcal{T}} F(\omega)$$

The power spectrum of each is $|F(\omega)|^2$, since

$$e^{-j\omega\mathcal{T}} F(\omega) \cdot e^{j\omega\mathcal{T}} F(\omega)^* = |F(\omega)|^2$$

Therefore, in the frequency domain, the signals are identical with respect to their power spectrums. Now a measure of the similarity coefficient between power spectra is necessary and the formula is shown below.

$$s(\vec{x}, \vec{y}) = \frac{\vec{x}^t \vec{y}}{\vec{x}^t \vec{x} + \vec{y}^t \vec{y} - \vec{x}^t \vec{y}}$$

where t: vector transpose

$s(\vec{x}, \vec{y})$: similarity coefficient between two vectors $\vec{x}$ and $\vec{y}$.

The data we will be acquiring is digital in nature and therefore vector notation is used. $\vec{x}$ can be a reference power spectrum stored as a sequence of sampled values. $\vec{y}$ can be a power spectrum of the comparison signal obtained from the system under consideration.

First we note that all values of the power spectrum will be positive. Therefore $s(\vec{x}, \vec{y})$ will always be positive. Secondly, if $\vec{y} = \vec{x}$, then $s(\vec{x}, \vec{y}) = 1$ which is its maximum value. If $\vec{y} = 0$, then $s(\vec{x}, \vec{y}) = 0$ which is the minimum value and also shows the complete dissimilarity of the vectors.

The similarity coefficient analysis developed so far was used for detecting the signal change ("delta signal") on the offshore K-joint model. The reference signals were acquired from each data acquisition location before being loaded and stored as an RF waveforms in the computer. The signals obtained during cyclic loading were used for the comparison signals as mentioned earlier. The power spectrums of both the reference and the comparison signals were extracted and normalized and used for $\vec{x}$ and $\vec{y}$ repsectively for the $s(\vec{x}, \vec{y})$ computation. Considering a typical power spectrum, we can notice that most of its energy is centered around its peak frequency,

Also from ultrasonic theory, we know that the energies belonging to the frequencies at the lower and upper ends of the spectrum are mainly due to noise. Therefore a similarity measure that weights the higher amplitudes near the peak frequency more than those at the extremes is required. Such a measure is the Tanimoto measure (8).

Computing the similarity coefficients, the following cases should also be considered. The same amount of skewness or shift of the spectra in the different directions, however, can not be distinguished from each other by above procedure. In other words, in Figure 5, both (a) and (b) may have the same magnitude in similarity coefficient if the entire spectra were compared directly. However, they might have entirely different physical characteristics. One possible way to avoid this confusion is by comparing the spectra section by section in smaller divisions as shown in Figure 5.

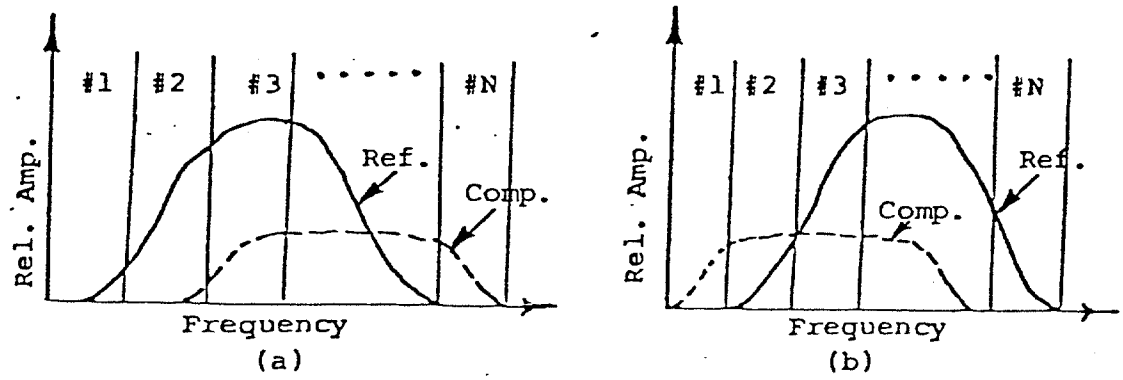

Figure 5. Sectionalized Spectra

According to the above concepts, each spectrum was divided into four smaller divisions as shown in Figure 6.

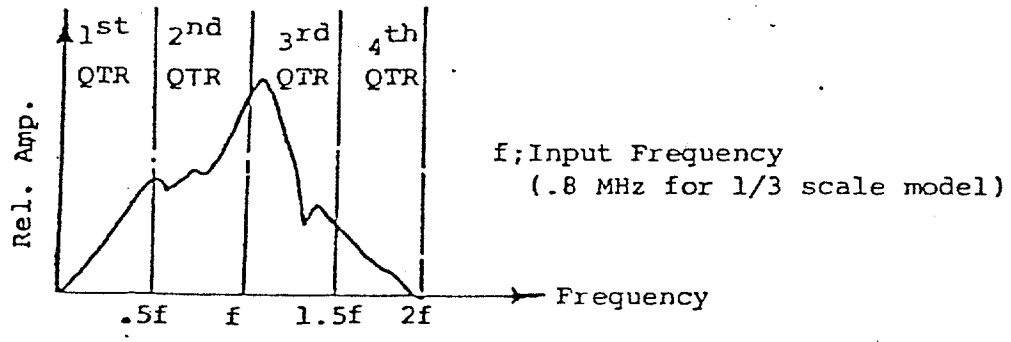

Figure 6. Frequency Ranges for Each Division of the Spectrum.

Finally, a series of curves(S vs. No. of fatigue cycles) for each data acquisition location were plotted as shown in Figure 10. Based on these curves, a decision algorithm was developed for the reliable damage detection. Consider a moving threshold average over all points previously recorded. Then consider a drop in the average threshold of greater than 20%. This indeed indicates that damage has taken place.

7. Phase I; 1/19 Scale K-joint Model Study

Two 1/19 scale K-joint models(2.75" O.D., .125" wall thickness) were fabricated at Drexel University. The global signals from six different locations were acquired using a set of 2.25 MHz transducers. The specific transducer positions were previously shown in Figure 3 and the data acquisition locations are shown in Figure 7 (Points 1 thru 6).

The signals without damage were acquired from each location and used as reference signals. For the flaw simulation, side drilled holes (starting from 1/16" in diameter) were machined sequentially in 1/64" increments. Ultrasonic signals were obtained from each size of the hole and stored in the storage device (floppy disks) for further signal processing.

Finally, the similarity coefficient was calculated for each size of the hole and each location using the stored data. The results of this study showed that there was a distinct drop in the similarity coefficient down to .8 with 3/32" diameter. A 3/32" diameter hole is about 1.2% of the total weld length (8 inches) around the node.

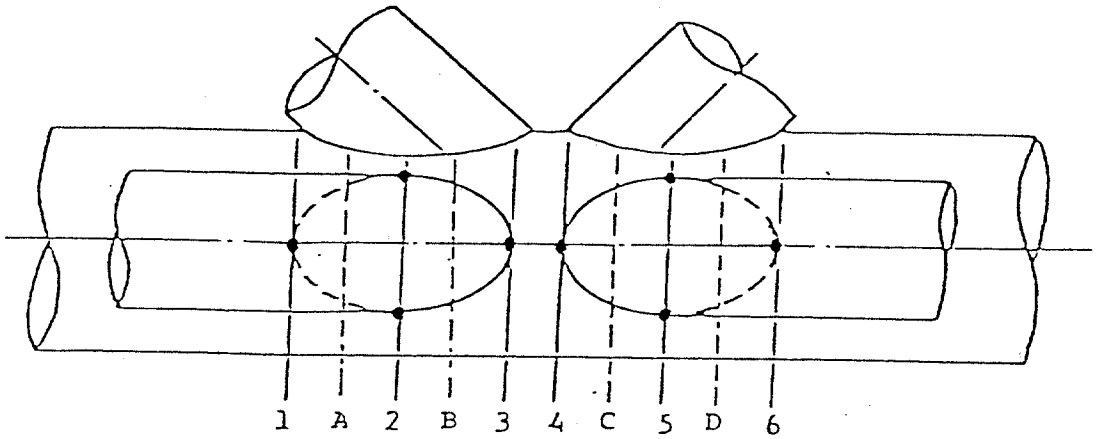

• : Flaw Locations
1 - 6 : Data Acquisition Points for 1/19 Scale K-Joint Model
A - D : Data Acquisition Points for 1/10 Scale K-Joint Model

Figure 7 . Data Acquisition Points and Flaw Locations for 1/19 and 1/10 scale K-joint models.

8. PHASE II; 1/10 SCALE K-JOINT MODEL STUDY

Two 1/10 scale K-joint models (5" O.D., .125" wall thickness) were also fabricated at Drexel University. The global signals from four different locations were acquired. The number of the data acquisition locations were reduced from six to four by considering the beam spread and the joint configuration as shown in Figure 7(A-D).

Under the assumption of linear relationship between the sound path distance and the sound energy loss, a set of 1 MHz transducers (transmitter and receiver) was selected for this model. Damages on the pipe weld were generated by saw cut starting from 1/2" in length in 1/8" increments. The same analysis as for the 1/19 scale model was carried out.

The results of this study showed that a 1 1/2" saw cut in length could be detected, and that there was a distinct drop in the similarity coefficient down to .7. A 1 1/2" saw cut is about 12% of the total weld length (13 inches) around the node.

9. PHASE III: 1/3 SCALE K-JOINT MODEL STUDY

A. Fatigue Test

A 1/3 scale K-joint model(18" O.D., 3/4" wall thickness) was built by the University of Maryland. Although the overall test protocol was basically the same as for the earlier phases, an actual fatigue test was carried out at NASA for improved damage simulation. The entire test bed is shown in Figure 8(a) and 8(b). A hydraulic pump was attached to the two lower legs of the K-joint model. Fatigue loading system was horizontal, unidirectional which made it easier to predict the crack initiation locations beforehand. The fatigue load was changed periodically in order to control the entire test period. The hydraulic loading pattern during the fatigue test on the 1/3 scale K-joint model is shown in Figure 9. Because the fatigue load was increased very rapidly after 40,000 cycles, the actual fatigue life on this period would be much longer than shown in the test results. The important concept of this test is, however, to see if any serious damage can be detected by ultrasonics before complete failure takes place.

According to the aforementioned scaling consideration of the K-joint model, four 800 kHz transducers were specially manufactured. Adapted shoes were also designed at Drexel University for the 1/3 scale K-joint model.

Seven different data acquisition locations were carefully chosen by analyzing the hot spots on the K-joint weld as shown in Figure 8(b). However, a major concern was at the positions #2, #4, #6 and #7 for this particular loading system, later proven by the ultrasonic global inspection technique.

In order to convince our test results, dye-penetrant test was also carried out simultaneously. Actual cracks after 39,600 cycles were shown in Figure 10.

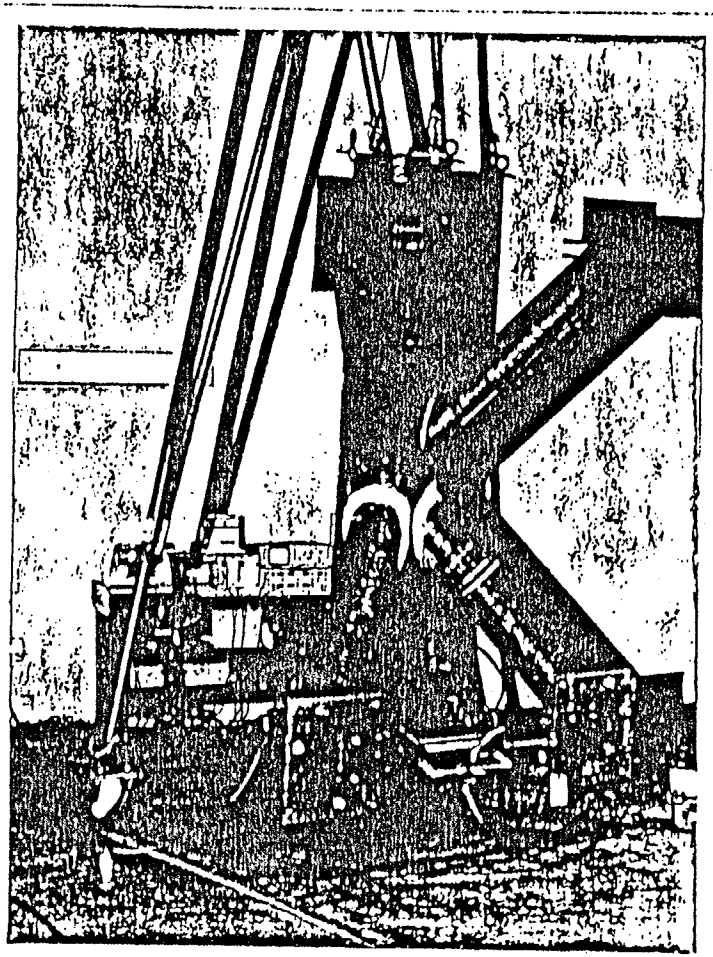

(a)

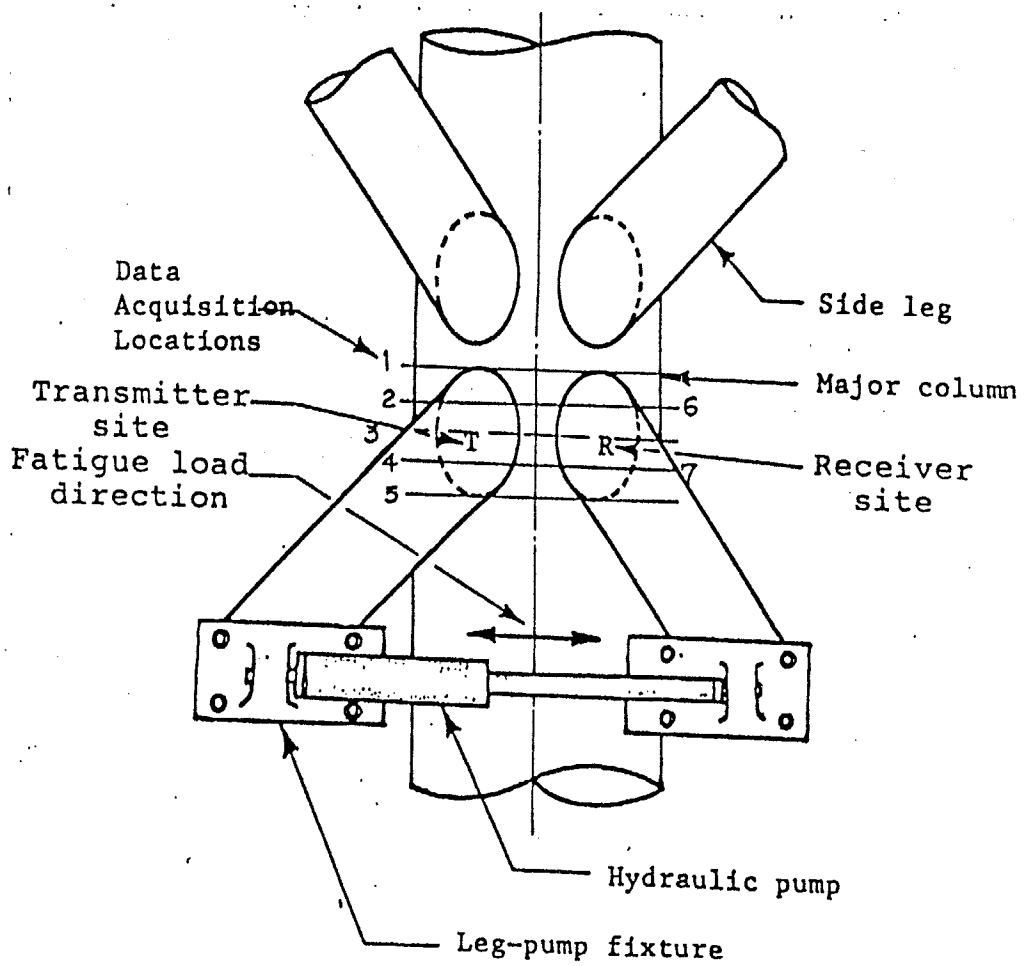

(b)

Figure 8. Fatigue Test Configuration for 1/3 Scale K-Joint Model

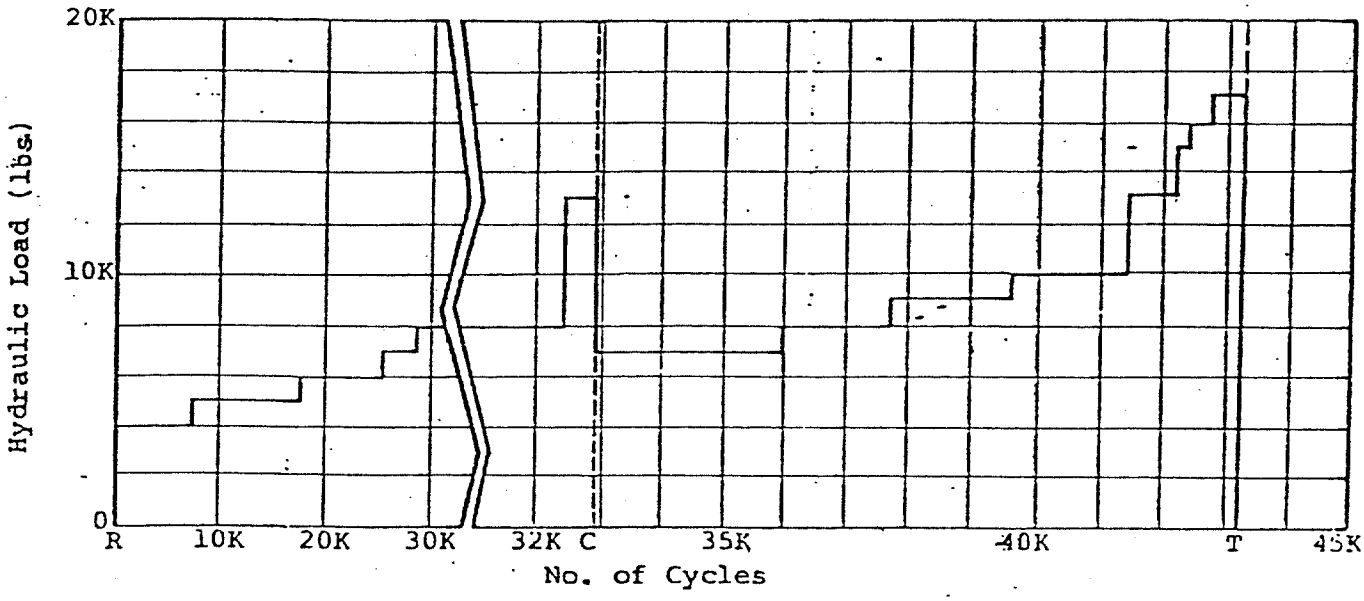

Note: C; Crack initiation point
T; Complete failure point
R; Starting Point of fatigue loading

Figure 9. Hydraulic Loading Pattern During the Fatigue Test on the 1/3 Scale K-joint Model

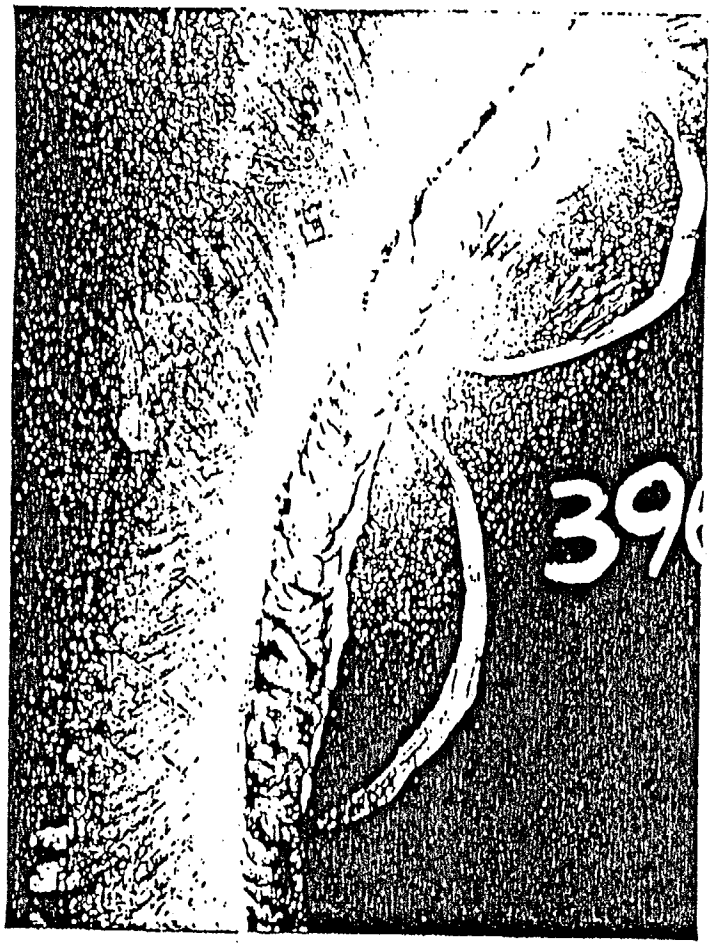

(a) Lower Left Leg
(2 1/2" and 3" Cracks)

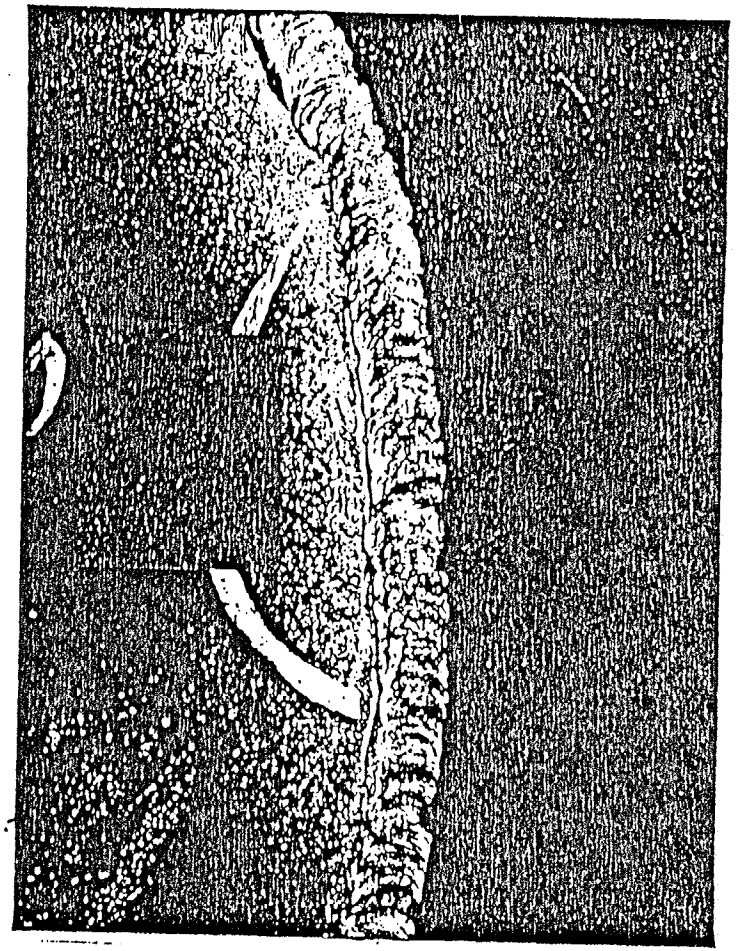

(b) Lower Right Leg
(1 1/2" and 2" Cracks)

Figure 10. Dye-Penetrant Test Results After 39600 Cycles.

B. Similarity Coefficient Analysis for 1/3 Scale K-Joint Model

As explained earlier, this mathematical expression thus allows us to compare the status of the K-joint weld integrity after loading(comparison signals) to the status before loading(reference signals).

The reference signal and the comparison signal are, however, not always in phase in time domain. Therefore, in order to eliminate the phase shift problem, a frequency spectrum analysis was carried out. Each spectrum was divided into 4 smaller quadrants for the similarity coefficient computation. A total of 35* S/N curves were plotted. Some of the best results are shown in Figure 11.

Note that the positions #6 and #7 are the reverse beam directions at the positions #2 and #4 respectively. As shown in the Figures, positions #2 and #4 where cracks occurred showed distinct drops after 41,400 cycles.

The percent remaining life, therefore, can be computed as follows;

$$R = \frac{C - P}{C} \times 100$$

Where R : % Remaining Life

C : Number of Cycles at the Complete Rupture

P : Number of Cycles at the Prediction

The earliest prediction of the damage in this approach was a 4.2% remaining life to the complete failure. The computation is shown below;

$$4.2\% = \frac{(43{,}192 - 41{,}400)}{43{,}192} \times 100$$

The crack length at the time of damage detection was 6 3/4"(17% of the entire weld length of the K-joint, 40").

Note: * See Table 3.

As shown in Table 3, using the entire portion of the spectrum to compute the similarity coefficients, 1% remaining life was predicted from the locations #2, #3 and #6. However, dividing into smaller divisions, we were able to detect the damage as early as 4.2% remaining life. The second quadrant of the spectrum (.4 MHz - .8 MHz) produces the best result.

The concept of the percent remaining life can be explained further as follows; Platforms are designed to meet both a maximum stress creteria and fatigue life creteria. A typical design philosophy for North Sea platforms, for example, where fatigue is important, sets the 100 year storm, showing 28 meter of average wave height, maximum stress at up to 80% of the yield strength with 25 years service life for fatigue assessment. Therefore, a 4.2% remaining life indicates more than a year before complete rupture of the K-joint, which shows enough period of time to repair the damage.

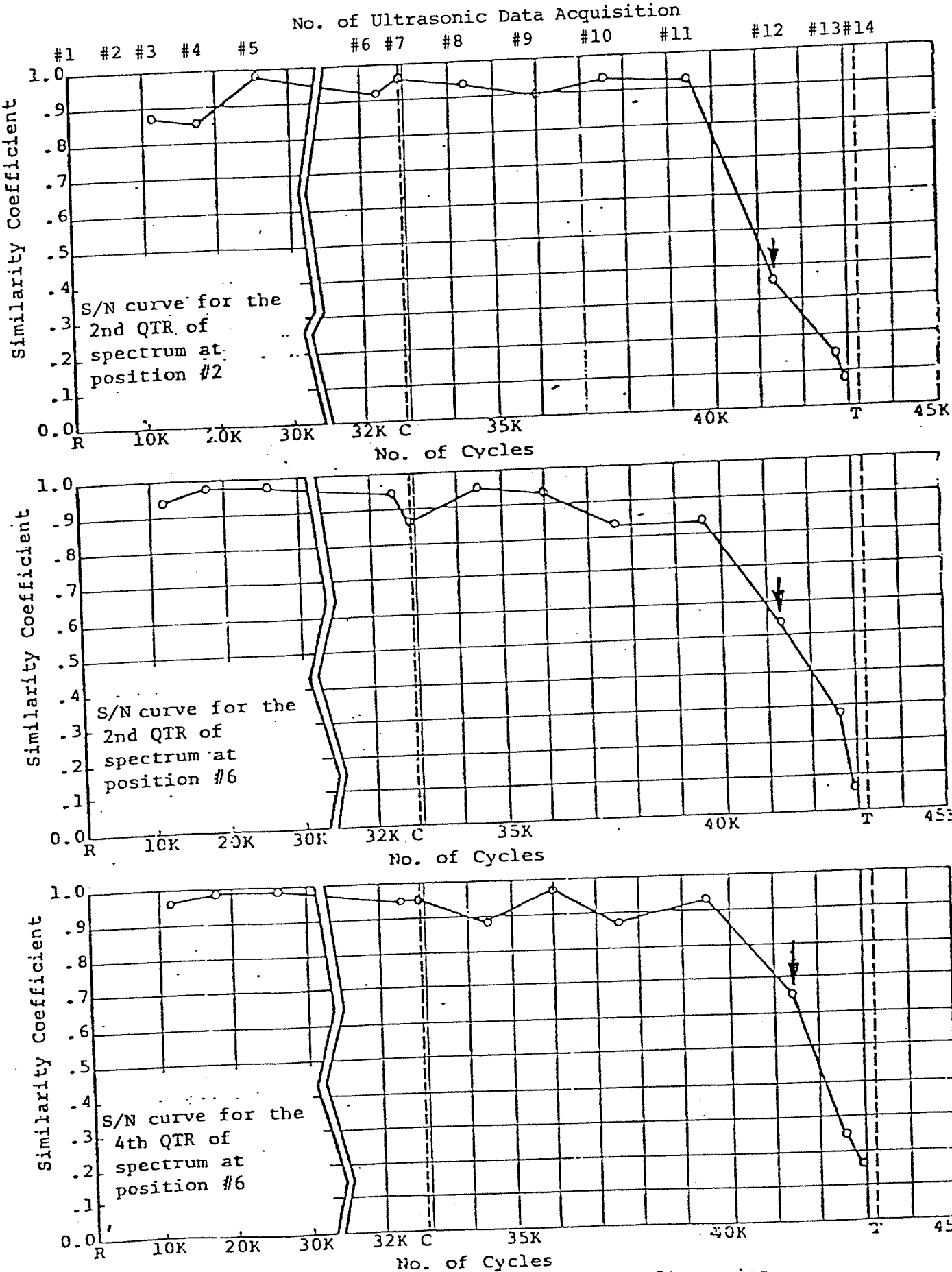

Note: ↓ The point of damage detection by ultrasonics

Figure 11. Typical S/N Curves(The three best results)

Table 3. % Remaining Life at The Time of Damage Detection on 1/3 Scale K-Joint Model Study.

Position	Total Spectrum	1st QTR	2nd QTR	3rd QTR	4th QTR
1	.5%	too noisy	N/A	.5%	N/A
2	1%	too noisy	4.2% *	1%	.5%
3	1%	too noisy	1%	1%	1%
4	N/A	too noisy	N/A	N/A	N/A
5	N/A	too noisy	N/A	N/A	N/A
6	1%	too noisy	4.2% *	1%	4.2% *
7	N/A	too noisy	.5%	N/A	N/A

Note; S/N curves of *'s are shown in Figure 11.
(5 Columns x 7 rows = 35 S/N Curves)

10. CONCLUSIONS

A feasibility study of damage detection with ultrasonics in K-joint model has been successfully carried out. Therefore, an ultrasonic global inspection technique could remove many of the difficult and time consuming factors as well as the total inspection cost of an offshore structure.

By proper implementation of the test protocol into compact, portable equipment for the field inspection, real time, remote analysis will be possible. This technique will not be affected by such environmental conditions as weather, water state, etc.

The conclusions are summarized below:

1. The feasibility study shows that a 4.2% remaining life can be predicted by using a decision algorithm as follows.

Consider a moving threshold average of over all points previously recorded. Then consider a drop in the average threshold of greater than 20%. This indeed indicates that damage has taken place. The second quarter of the spectrum produces the best results.

2. The optimum transducer frequency turned out to be between 250 KHz and 500 KHz for the full scale K-joint inspection (54" O.D., 3/4" wall thickness).

3. The scaling study showed that $.2 < \lambda/t < 1.0$ is the optimum range for resolution, sound path/$\lambda < 350$ is the acceptable range for penetration. Both of the above decision criteria are directly related to the transducer frequency and the pipe size.

11. RECOMMENDATIONS

Based on the experiance obtained throughout the entire project, the following recommendations for future research effort have been made.

1. Constant fatigue load should be applied throughout the fatigue test for improved performance.

2. Permanent attachment of the transducers on the outside surface of the pipe should be made for improved sensitivity.

3. Test in water should be conducted for better simulation of the environmental condition, because there is a considerable difference in sound energy attenuation across the different interface

4. A study on the implementation for field application should be made including data transmission, transducer mounting, number of transducer elements, transducer design (e.g. mosaic type design), etc.

12. ACKNOWLEDGEMENTS

We would like to thank the Office of Naval Research for their contractual support of this project. Also, we would like to thank Krautkramer-Branson, Inc. for the use of a KB-6000 and computer support, and finally, we would like to thank John B. Nestleroth and other students at Drexel University who helped on this project.

REFERENCES

1. Smart, J. S. III, "Corrosion Failure of Offshore Steel Platforms," Materials Performance, National Association of Corrosion Engineers, Vol. 19, No. 5, May 1980, pp. 41-48.

2. Krautkramer, Ultrasonic Testing of Materials, Springer-Verlag New York Inc., 1969.

3. Chen, C. H., Statistical Pattern Recognition, Hayden Book Company, Inc., Rochelle Park, New Jersey, 1973.

4. Schwartz, M. and Shaw, L., Signal Processing, Discrete Spectral Analysis, Detection, and Estimation, McGraw-Hill Book Company, New York, 1975.

5. "The North Sea's Worst Disaster," Ocean Industry, Vol. 15, No. 4, April 1980, p. 176.

6. "Marine Growth on Maui Platform," Offshore Engineer, April 1980, p. 145.

7. "Ultrasonic Camera for Underwater Inspection," Offshore Engineer, April 1980, p. 15.

8. Tou, J. T. and Gonzalez, R. C., Pattern Recognition Principles, Addison-Wesley Publishing Company, Reading, Massachusetts, 1974.

9. Avioli, M. J., Utilization of Signal Processing and Pattern Recognition for the Advancement of Ultrasonic Nondestructive Testing, Ph. D. Theses Dissertation, Dept. of Mechanical Engineering, Drexel University, June 1981.